Physics AUC, vol. 24, 80-96 (2014)

Modeling of arbitrary electromagnetic beam propagation in terms of asymptotic wave methods

Christos Tsironis, Aristeidis Papadopoulos
Division of Electromagnetics, Electrooptics and Electronic Materials,
School of Electrical and Computer Engineering,
National Technical University of Athens, 157 44 Athens, Greece

Abstract

The mainstream in the theory and applications of electromagnetic wave propagation in kinetic media is oriented to frequency-domain asymptotic methods, assuming linear dielectric response, where a solution of the Vlasov-Maxwell problem is more feasible. Even for the cases when the short-wavelength limit breaks down, asymptotic methods are in principle robust in still providing a meaningful solution. The most popular of these methods are the ray and beam tracing techniques, which reduce the (partial differential)full-wave equation to a set of ordinary differential equations. In most computer applications, the ray/beam tracing codes are configured to follow Gaussian beams only. In this paper, the extension of such schemes to include more complicated, arbitrary beams is presented. As a first step, the decomposition of the beam propagation into the one of properly configured ray/beam modes is analyzed. Then, a generalization of the Gaussian beam parameters and of the amplitude transport of the modes is formulated. As an instructive application, we solve the propagation of non-Gaussian electron-cyclotron beams in a plasma with stratified magnetic geometry and kinetic pressure.

1 Introduction

The propagation of electromagnetic waves in inhomogeneous media is described by the vector wave equation [1]. In principle, the derivation of a full-wave solution is very hard, because this equation is partial differential and a constitutive relation for the medium current response must be provided. In cases where the wavelength is small compared to the scale length of inhomogeneity of the medium, a simplification is achieved by employing frequency-domain asymptotic methods: Ray tracing (geometric optics) [2], quasi-optical ray/beam tracing [3, 4] or paraxial Wentzel-Krammers-Brillouin beam tracing [5]. These methods, initially intended for plasma applications but indeed being more general, exploit an asymptotic series expansion of the solution sought in a neighborhood of the considered location and time, and solve the equations emanating from the separation of terms of different orders [6].

Such "corpuscular" description of the propagation, in terms (among others) of a bundle of rays continuously refracted by a medium slowly-varying in time/space, makes the problem resemble to the motion of a particle deflected by a scalar potential [7]: The rays correspond to the particle trajectories and the wave vector and frequency correspond to

the particle momentum and energy. In particular, both of the latter wave properties depend on the position along the ray in the same way as the particle momentum and energy depend on time; thus, one refers to local wave vector and local frequency in this framework. Moreover, the wave phase corresponds to the action of the equivalent mechanical system, and thus satisfies a Hamilton-Jacobi equation.

In ray and beam tracing analysis, the solution is obtained through ordinary differential equations emerging from a canonical formalism, where the wave dispersion function plays the role of the Hamiltonian. For problems related to plasmas, it is customary to assume fluid-like (i.e cold plasma) dispersion for the Hamiltonian function, where the medium dielectric tensor is derived in terms of the linear theory of plasma oscillations in the presence of small-amplitude waves [8]. There are several ray and beam tracing codes that implement the schemes described above (see e.g. [9, 10, 11]), and the results obtained are in reasonable agreement with the experiment (details can be found in [12, 13]) apart from cases where the short-wavelength limit breaks down, e.g. due to steep density gradients [14] or cut-offs, or where the system has gone beyond the linear threshold of wave-particle interaction [15, 16].

In the majority of applications, especially to tokamak fusion, high-frequency waves with narrow profile of the electric field amplitude and an initial focusing of the wave-front (i.e. beam-shaped) are considered [13, 17]. The advantages of this option are numerous; just to mention, in plasma heating experiments the localization of wave-particle resonant absorption is increased, in diagnostics the investigated region is made as small as possible, and in magnetohydrodynamic stability control an alignment is achieved with the phases of the instabilities. The state-of-the-art in theory and experiment is mainly based on Gaussian-shaped beams. Their employment is preferable because of their low Ohmic losses in the wave transmission lines, and also due to the fact that they allow an easy coupling to waveguide modes; furthermore, such wave structures are easy to model in theoretical and numerical investigations.

It is the case, however, that the beam, before entering the plasma region, already does not have a Gaussian profile shape. This is usually an unwelcome effect, owed to a misalignment of the wave launching system or to a deformation of the materials involved due to extreme heat load (e.g. when the wave power density attains large values). In the latter case then, a non-Gaussian beam profile may be intentionally set up in order to reduce the power density on the optical structures between the wave source, the transmission line and the plasma vessel. Furthermore, in the plasma, a modification of the initial Gaussian beam might occur due to localized absorption, non-local redistribution of energy by resonant particles along the magnetic field lines, vivid focusing and/or strong wave interference.

The coupling of non-Gaussian beams to the plasma is a part of the literature that has not been significantly studied (the reader is referred to [18] and the comments in [5]). In this paper, models based on the asymptotic methods are formulated for the calculation of the propagation of arbitrary beams in inhomogeneous anisotropic media. First, the sequence for following arbitrary beams in terms of ray tracing, as a bunch of independent rays carrying the non-Gaussian power profile, and paraxial beam tracing, as a central ray bound to scalar functions of the beam geometry, is established. Then, the beam description through well-known parameters, like e.g. the width and the curvature radius, is recovered by generalizing the parameters already defined for Gaussian beams. As an example case, the propagation of a non-Gaussian electron-cyclotron beam in simplified plasma geometry is calculated.

The structure of the paper is as follows: In Section 2 the ray and beam tracing

techniques are briefly presented, and in Section 3 the sequence of tracing the beam path and amplitude/power in terms of the two different techniques is analyzed and explained. In Section 4, a set of generalized beam parameters are introduced in the specific setup of each model, and in Section 5 the merits of the two models are uncovered with the application in an example problem. Finally, in the last section, conclusions are made and the future targets of our modeling are discussed.

2 Frequency-domain asymptotic wave methods

The evolution of any type of electromagnetic field in all kinds of media is described by Maxwell's equations. Especially for wave propagation, a manipulation of these equations yields the vector wave equation, a separate one for the electric and the magnetic field, which relates more straightforwardly the electromagnetic fields to the response of the medium where the wave propagates. The general form of the wave equation for the complex electric field vector $\overline{\mathbf{E}}$ reads [8]

$$\nabla^2\overline{\mathbf{E}}(\mathbf{r},t) - \frac{1}{c^2}\frac{\partial^2\overline{\mathbf{E}}(\mathbf{r},t)}{\partial t^2} = \frac{\nabla\rho(\mathbf{r},t)}{\varepsilon_0} + \mu_0\frac{\partial\bar{\mathbf{j}}(\mathbf{r},t)}{\partial t}, \tag{1}$$

with ρ, $\bar{\mathbf{j}}$ respectively the electric charge and current volume densities in the medium.

With the intention to achieve a simplification to the solution of Equation (1) in problems related to propagation in magnetized plasmas with slow spatiotemporal variation, we consider a medium which is, in principle, time-independent, weakly inhomogeneous and anisotropic. Then, the wave electric field can be considered of the form $\overline{\mathbf{E}}(\mathbf{r},\mathbf{t}) = \overline{\mathbf{E}}(\mathbf{r})\exp(-\mathbf{i}\omega\mathbf{t})$ (ω is the wave frequency), whereas the medium response may be expressed in terms of a spatially inhomogeneous dielectric tensor $\hat{\varepsilon}$, obtained by introducing a spatial dependence to the corresponding quantities that enter the dielectric tensor formula of the homogeneous plasma (see [8] for details). In that frame, the general wave equation reduces to the vector Helmholtz equation [1]

$$\nabla\times[\nabla\times\overline{\mathbf{E}}(\mathbf{r})] - \frac{\omega^2}{c^2}\hat{\varepsilon}(\mathbf{r},\omega)\cdot\overline{\mathbf{E}}(\mathbf{r}) = 0. \tag{2}$$

Historically, the first method to provide an asymptotic solution of (2) is ray tracing, a product of geometric optics theory [2]. Within this technique, the wave field is expressed in the eikonal form, which is actually a generalization of the standard ansatz for the plane wave that includes the weak inhomogeneity [6]

$$\overline{\mathbf{E}}(\mathbf{r}) = \overline{\mathbf{A}}(\mathbf{r})\exp[i\kappa s(\mathbf{r})]. \tag{3}$$

In the above relation, $\overline{\mathbf{A}}$ is the electric field amplitude, s is the eikonal function that generalizes the plane-wave phase $\mathbf{k}\cdot\mathbf{r}$ for weakly inhomogeneous media, and $\kappa = \omega L/c \gg 1$ is the short-wavelength limit parameter, with L being the typical inhomogeneity scale length of the medium, defined as the maximum of the average normalized gradients among the parameters affecting propagation (i.e. entering the dispersion relation). The connection of the eikonal function and the wave-vector is $\mathbf{k} = \kappa\nabla s$.

For each ray, one can determine the "backbone" of the wave field by means of a set of ordinary differential equations that give the variation of the phase and the amplitude along the ray. These are obtained by exploiting an asymptotic series expansion of the

solution form assumed in a neighborhood of the considered position

$$\overline{\mathbf{A}} = \sum_m \overline{\mathbf{A}}_{\mathbf{m}} \kappa^{-m}, \tag{4}$$

inserting (3), (4) in (2) and separating terms of different order in the parameter κ^{-1}. From the emerging equations, the one of zero-order describes the evolution of the wave phase in space and involves the Hermitian part of the dielectric tensor

$$\left[\kappa^2(-k^2\widehat{\mathbf{I}} + \mathbf{kk}) + \hat{\varepsilon}^H\right] \cdot \overline{\mathbf{A}}_{\mathbf{0}} \equiv \widehat{\mathbf{\Lambda}} \cdot \overline{\mathbf{A}}_{\mathbf{0}} = 0. \tag{5}$$

The solvability condition of Equation (5) reads $\det[\widehat{\mathbf{\Lambda}}] \equiv D = 0$ and is actually the linear dispersion relation for the wave, involving the dispersion tensor $\widehat{\mathbf{\Lambda}}$. The specific relation may be viewed as a Hamilton-Jacobi equation with respect to s; in this manner, it is possible to derive Hamiltonian ray equations which trace the evolution of the wave trajectory and the wave-number along the ray

$$\frac{d\mathbf{r}}{d\tau} = \frac{\partial D}{\partial \mathbf{k}}, \tag{6a}$$

$$\frac{d\mathbf{k}}{d\tau} = -\frac{\partial D}{\partial \mathbf{r}}. \tag{6b}$$

Moreover, the first-order equation provides the wave amplitude transport (i.e. the evolution of the amplitude along the ray)

$$\frac{d|\overline{\mathbf{A}}_{\mathbf{0}}|^2}{d\tau} = -\left(\nabla \cdot \mathbf{v_g} + 2\gamma\right)|\overline{\mathbf{A}}_{\mathbf{0}}|^2, \tag{7}$$

where $\gamma = \bar{\mathbf{e}}^* \cdot \hat{\varepsilon}^A \cdot \bar{\mathbf{e}}$ is the absorption coefficient, describing the wave power damping by the medium, and $\bar{\mathbf{e}}$ the unitary (complex) polarization vector (hence $\overline{\mathbf{A}}_{\mathbf{0}} = A_0\bar{\mathbf{e}}$). Equation (7) implies that the wave energy propagates in the direction of the group velocity $\mathbf{v_g} \propto \partial D/\partial \mathbf{k}$, and also that the absorption is proportional to the projection of the anti-Hermitian part of the dielectric tensor onto the polarization vector.

The ray tracing approach provides a very effective solution to the wave equation within the short-wavelength limit, with the caveat, however, that wave phenomena related to diffraction and interference are not included in the description. This comes from the fact that, in the conventional formulation of geometric optics, such effects appear in the higher-order equations, which are cumbersome to treat and are left out of the picture (for more information, the reader is pointed to [19]). In situations where focused or collimated beams are involved, and therefore diffraction cannot be neglected, ray tracing computations lead to physical inconsistencies near the beam focus point (as seen in Figure 1a). For that reason, theoretical tools that upgrade geometric optics have been developed for the consistent modeling of the diffractive variation of the beam width. These are complex geometric optics and paraxial beam tracing, which are also referred to as quasi-optical methods.

The former technique introduces that the wave phase is complex-valued, i.e. $\bar{s} = s + i\phi$, with the imaginary part being related to the electric field profile transverse to the beam propagation. The ansatz for $\overline{\mathbf{E}}$ is modified to [3, 4]

$$\overline{\mathbf{E}}(\mathbf{r}) = \overline{\mathbf{A}}(\mathbf{r}) \exp[i\kappa\bar{s}(\mathbf{r})] = \overline{\mathbf{A}}(\mathbf{r}) \exp[-\kappa\phi(\mathbf{r})] \exp[i\kappa s(\mathbf{r})], \tag{8}$$

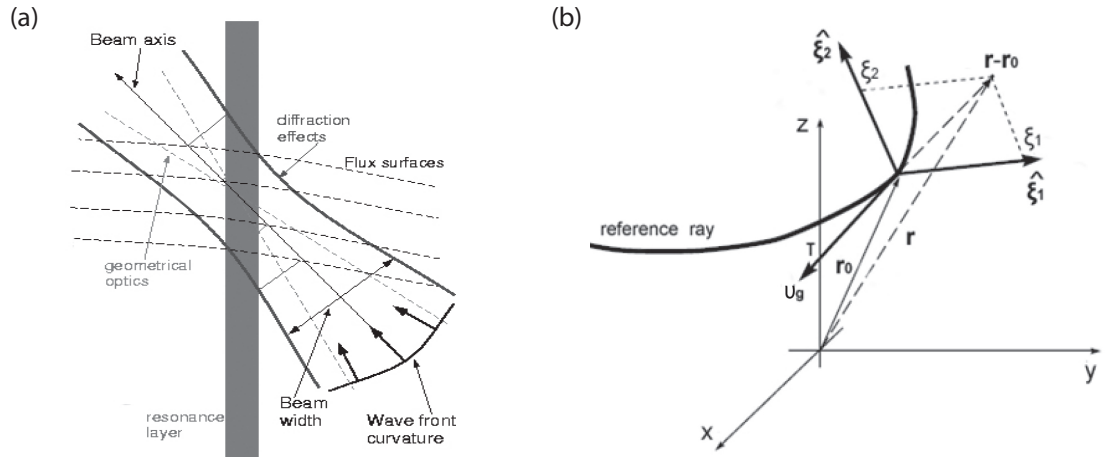

Figure 1: (a) Illustration of the wave beam representation in terms of the asymptotic methods, (b) The local beam coordinate system (τ, ξ_1, ξ_2) (figures reprinted from Reference [10]).

where the imaginary wave-vector $\mathrm{Im}(\bar{\mathbf{k}}) = \kappa \nabla \phi$ is, according to the above definition, normal to $\mathbf{v_g}$. A new scale length comes into play, the beam width w, which is intermediate to the wavelength λ and L since, according to the Fresnel condition $w^2 \geq \lambda L$, $\mathrm{Im}(\bar{\mathbf{k}}) \propto w^{-1}$ is of order $\kappa^{-1/2}$ with respect to $\mathrm{Re}(\bar{\mathbf{k}})$. The corresponding complex solutions can be obtained in two different ways: First, a set of Hamiltonian equations describing modified rays is derived, followed by a Taylor expansion in the complex dispersion relation according to $\mathrm{Im}(\bar{\mathbf{k}}) \ll Re(\bar{\mathbf{k}})$. The resulting dispersion function consists only of real terms, the zero-order term of geometrical optics and a higher-order term that describes diffraction [3]. On the other hand, one can extend the equations in complex space by means of the analytical continuation of D, and then derive a geometric optics solution in complex space. Thereafter, the physical wave field is obtained by evaluating the solution at a real-valued observation point (details in [4]).

The third approach is the paraxial beam tracing method, which combines the simplicity of ray tracing with the provision of a description of diffractive effects. There, the electric field has the same form as in quasi-optics theory, however the amplitude series expansion implicitly contains the intermediate order $\kappa^{-1/2}$ [5]

$$\overline{\mathbf{A}} = \sum_{m,n} \left[\Phi_{m,n} \overline{\mathbf{A_0}} - i\kappa^{-1/2} \sum_j \frac{\partial \Phi_{m,n}}{\partial \xi_j} \overline{\mathbf{A_1^j}} - \kappa^{-1} \left(\frac{1}{2} \sum_{j,l} \frac{\partial^2 \Phi_{m,n}}{\partial \xi_j \partial \xi_l} \overline{\mathbf{A_2^{jl}}} - i \Phi_{m,n} \overline{\mathbf{A_3}} \right) \right]. \quad (9)$$

The function $\Phi_{m,n}(\xi_1, \xi_2) = \phi_m(\xi_1)\phi_n(\xi_2)$ describes the transverse beam profile on the basis of orthogonal wave modes with base function $\phi_n(x) = \exp(-x^2/2) H_n(x)$ (H_n the normalized Hermite polynomials). In the above, a local system of dimensionless beam coordinates (τ, ξ_1, ξ_2) has been introduced, visualized in Figure 1b, where τ is along and ξ_1, ξ_2 across the propagation direction. The curve $\mathcal{R}\{\xi_1 = \xi_2 = 0\}$ is a geometric-optics ray that describes the center of gravity of the beam, and the electric field profile spans across $\mathcal{R}$ according to the unitary quadratic form $\phi = \delta_{i,j} \xi_i \xi_j / 2$.

The complex phase of the wave field may be expanded in Taylor series around $\mathcal{R}$

$$\bar{s} = \bar{s}(\mathcal{R}) + \sum_\alpha \frac{\partial \bar{s}}{\partial x_\alpha} \left[x_\alpha - x_\alpha(\mathcal{R}) \right] + \frac{1}{2} \sum_{\alpha,\beta} \frac{\partial^2 \bar{s}}{\partial x_\alpha \partial x_\beta} \left[x_\alpha - x_\alpha(\mathcal{R}) \right] \left[x_\beta - x_\beta(\mathcal{R}) \right], \quad (10)$$

which is the rationale behind the characterization of this method as "paraxial". The coefficients $\bar{s}_\alpha = \partial\bar{s}/\partial x_\alpha$ are zero due to the normality of the wavenumber on the group velocity, and $\bar{s}_{\alpha,\beta} = \partial^2\bar{s}/(\partial x_\alpha \partial x_\beta) = s_{\alpha,\beta} + i\phi_{\alpha,\beta}$ are determined by ordinary differential equations emerging from the terms of order $\kappa^{-1/2}$ in (9)

$$\frac{d\bar{s}_{\alpha,\beta}}{d\tau} = -\frac{\partial^2 D}{\partial x_\alpha \partial x_\beta} - \sum_\gamma \left[\frac{\partial^2 D}{\partial x_\beta \partial k_\gamma}\bar{s}_{\alpha,\gamma} - \frac{\partial^2 D}{\partial x_\alpha \partial k_\gamma}\bar{s}_{\beta,\gamma} \right] - \sum_{\gamma,\delta} \frac{\partial^2 D}{\partial k_\gamma \partial k_\delta}\bar{s}_{\alpha,\gamma}\bar{s}_{\beta,\delta}. \tag{11}$$

The coefficients $s_{\alpha,\beta}$ relate to the curvature radius ($\propto r_c^{-1}$), whereas $\phi_{\alpha,\beta}$ relate to the beam width ($\propto w^{-2}$). The equation for the amplitude transport is similar to (7), however here absorption is calculated on $\mathcal{R}$ but refers to the whole beam. In that frame, one employs the amplitudes $\overline{C}_{m,n} = A_0 \exp(i\Theta_{m,n})$, each one of which is the geometric-optics amplitude excluding the phase shift $\Theta_{m,n}$ over $\mathcal{R}$, given by [18]

$$\frac{d\Theta_{m,n}}{d\tau} = \left(m + \frac{1}{2}\right) \sum_{\alpha,\beta} \frac{\partial^2 D}{\partial k_\alpha \partial k_\beta} \frac{\partial \xi_1}{\partial x_\alpha} \frac{\partial \xi_1}{\partial x_\beta} + \left(n + \frac{1}{2}\right) \sum_{\alpha,\beta} \frac{\partial^2 D}{\partial k_\alpha \partial k_\beta} \frac{\partial \xi_2}{\partial x_\alpha} \frac{\partial \xi_2}{\partial x_\beta}. \tag{12}$$

3 Asymptotic solution for arbitrary wave beams

The description of arbitrary wave beam structures in terms of the superposition of simpler wave modes, compatible with the solution provided by the asymptotic methods, will be of assistance in following the propagation of generic beam profiles, as e.g. the one of a properly set-up bunch of ray-based or Gaussian-like modes. The results may be employed in the modeling of the wave power absorption in the plasma taking into account the modifications of the profile shape, due to localized absorption, in terms of the generation of higher-order modes which exchange energy among them. Such a model, in combination with advanced asymptotic codes like e.g. TORBEAM [10], may provide an improved description of the propagation, absorption and current drive in many cases of interest for tokamak plasma experiments.

The first step in this direction is to formulate a theoretical method, oriented to numerical applications, for the analysis of the arbitrary electric field profile into simpler components relevant to the asymptotic solution method at hand (ray or beam tracing). The two asymptotic methods, as seen also in the previous section, appear a notable difference in the description of the electric field vector: In ray tracing, each wave structure (i.e. the ray) is assumed to be a localized plane wave carrying all the wave power assigned at the launch point, whereas in beam tracing the wave is modeled as a central ray accompanied by scalar functions for the beam width and the curvature of the wavefront. These facts, together with the overall mathematical properties of each asymptotic method, should be considered in order to reach, per case, an optimal decomposition of the non-Gaussian beam.

We start with the paraxial beam tracing technique, where any wave beam is readily expressed as a superposition of Gaussian-Hermite modes [5]. With reference to the previous section, the ansatz for the spatial part of the electric field is written as

$$\overline{\mathbf{E}}(\mathbf{r}) = \bar{\mathbf{e}}(\mathbf{r}) \exp[i\kappa s(\mathbf{r})] \sum_{m,n} C_{m,n}(\mathbf{r}) \exp[-i\Theta_{m,n}(\mathbf{r})]\, \phi_m[\xi_1(\mathbf{r})]\phi_n[\xi_2(\mathbf{r})]. \tag{13}$$

As seen from (13), the amplitude of the electric field consists of two parts: The first one, essentially the function $\Phi_{m,n}$, determines the transverse distribution of the field amplitude

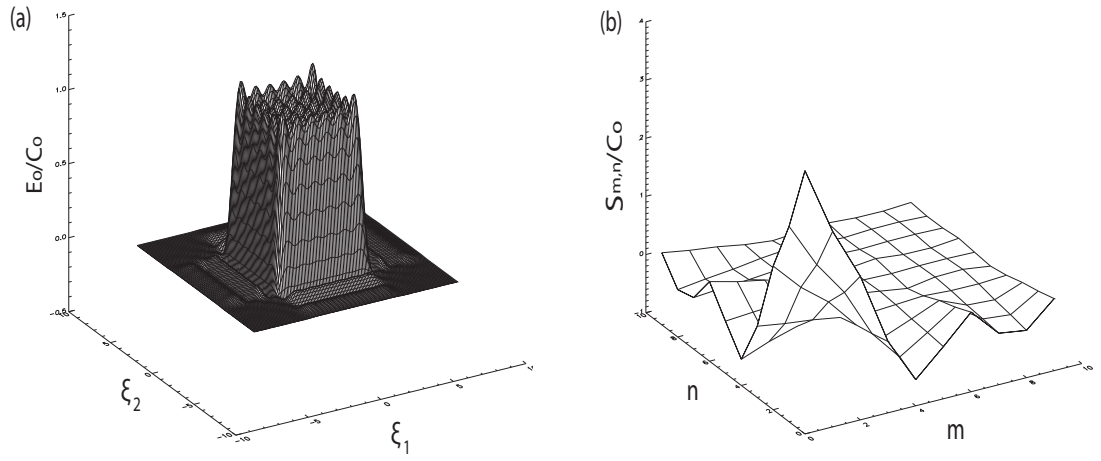

Figure 2: (a) Normalized amplitude profile of a two-dimensional square beam, as reconstructed using $MN = 20 \cdot 20 = 400$ modes. (b) Normalized coefficients of the Gaussian-Hermite modes, corresponding to the previous expansion, as a function of the mode indices.

in space (i.e. the beam profile). It is apparent that the amplitude decreases rapidly when moving outwards from the beam axis, a statement for the localization of the beam. On the other hand, the phase-shifted coefficients $\overline{S}_{m,n} = C_{m,n} \exp(-i\Theta_{m,n})$ have to do with the intensity of the beam, or, else said, with the energy density of the wave field; the exact connection is $U_E = \sum_{m,n} |\overline{S}_{m,n}|^2 = \sum_{m,n} |C_{m,n}|^2$. One has to notice also that, within this description, all the modes have the same polarization and generalized phase, as these are characteristics of the central ray.

For our purpose of decomposing the beam into simpler modes, the electric field may be cast in the form $\overline{\mathbf{E}} = \overline{E}_0 \exp(i\kappa s)\mathrm{Re}(\overline{\mathbf{e}})$, with E_0 the complex amplitude

$$\overline{E}_0(\xi_1, \xi_2) = \sum_{m,n} \overline{S}_{m,n} \phi_m(\xi_1) \phi_n(\xi_2). \tag{14}$$

It is trivial to understand that, apart from describing the evolution of the wave energy, the coefficients $\overline{S}_{m,n}$ contribute also to the exact shape of the beam profile as statistical weight coefficients. For obtaining the beam tracing solution when a certain type of input for the wave electric field is given, the coefficient values of the representing modes for this initial field should be calculated; then, together with the phase and polarization, their values may be found at each propagation instant by solving the amplitude transport equation per mode, and the solution is complete.

The coefficients of the series approximation given in (14) are computed from the generalized Fourier relation stemming from the orthogonality of the base functions [20]

$$\overline{S}_{m,n} = \int_{-\infty}^{\infty} \overline{E}_0(\xi_1, \xi_2) \phi_m(\xi_1) \phi_n(\xi_2) d\xi_1 d\xi_2. \tag{15}$$

Due to the phase difference existing between the propagating modes, one cannot determine directly from the initial amplitude $\overline{E}_0$ the values $\overline{C}_{mn}$, but only their phase-shifted versions $\overline{S}_{m,n}$. Furthermore, in practical applications, it is not possible to include the required, according to theory, infinite number of terms in the series expansion. In this case, one may resort to Bessel's inequality and define an "error function" for checking the accuracy

of the series approximation

$$\mathcal{D}_E(m,n) = \sum_{m,n} |\overline{S}_{m,n}|^2 - \int_{-\infty}^{\infty}\int_{-\infty}^{\infty} |\overline{E}_0(\xi_1,\xi_2)|^2 d\xi_1 d\xi_2 \leq 0. \tag{16}$$

As the number of terms increases, the amplitude sum should approach the value of the integral, and the error should proceed towards zero.

As an example, we consider the decomposition of a real-valued, square-shaped profile in two dimensions, represented in the form

$$E_0(\xi_1,\xi_2) = C_0[h(\xi_1+d) - h(\xi_1-d)][h(\xi_2+d) - h(\xi_2-d)], \tag{17}$$

which actually means that the electric field E_0 is nonzero only in the cubic box $\{[-d,d] \times [-d,d]\}$ around the propagation. In the previous relation, d is the half-width of the square profile, normalized by the same factor as the transverse coordinates, and $h(x)$ is the Heaviside step function [20]. By inserting (17) into (15), and using also the mathematical expression for the Gauss-Hermite base functions, the real-valued coefficients for the specific expansion are obtained

$$S_{m,n} = C_0 \int_{-d}^{d} \exp\left(-\xi_1^2/2\right) H_m(\xi_1) d\xi_1 \int_{-d}^{d} \exp\left(-\xi_2^2/2\right) H_n(\xi_2) d\xi_2. \tag{18}$$

The integrals on the right-hand side of (18) are of the same form and can be calculated analytically for certain values of n, but not also represented in a general analytic form. Another way to proceed with this calculation is through numerical methods.

In Figure 2 we show the results of the numerical solution for the square profile decomposition and reconstruction by a finite number of modes ($M \cdot N = 20 \cdot 20 = 400$ modes) with $d = 4$, $C_0 = 1$. From the reconstructed profile one concludes that the model is very efficient, except near the discontinuity planes $\pm d$. In Figure 2b, the expansion coefficients (normalized to C_0), are plotted as a function of m, n. The higher-order modes are found to have very small coefficients and not playing an important role in the reconstructed beam. The error $\mathcal{D}_E$ falls under 1% for $M, N > 10$, which means sufficient accuracy in this region. Notice here also that, since the beams studied are localized in space, the theoretical requirement for integration to infinity is overcome and the integration limits can be cut-off, without error, at sufficient distances.

Having the ability to decompose the launched waveform into beam-tracing compatible modes and to reconstruct the field along propagation, brings the solution pursuit to the point where all required quantities in (13) should be computed, namely $\bar{\mathbf{e}}$, s, $\overline{C}_{m,n}$ and $\Theta_{m,n}$. According to the aforementioned, the computation is straightforward; the only thing to keep in mind, in solving the amplitude transport equations, is that the absorption coefficient depends on the wave-vector which is different for each mode. In specific, the following relation holds [18]

$$\mathbf{k_{m,n}} = \nabla(\kappa s - \Theta_{m,n}) = \mathbf{k} - \frac{d\Theta_{m,n}}{d\tau}\nabla\tau, \tag{19}$$

where $\nabla\tau$ is computed from the reciprocal of the ray-tracing equation involving $d\mathbf{r}/d\tau$. The absorption coefficient can be evaluated directly from analytical models [21] or by solving the hot plasma dispersion relation as e.g. done in [9].

Within the ray tracing approach now, the situation is much more simple: The wave beam can be represented as a bunch of rays, initialized properly in order to shape the

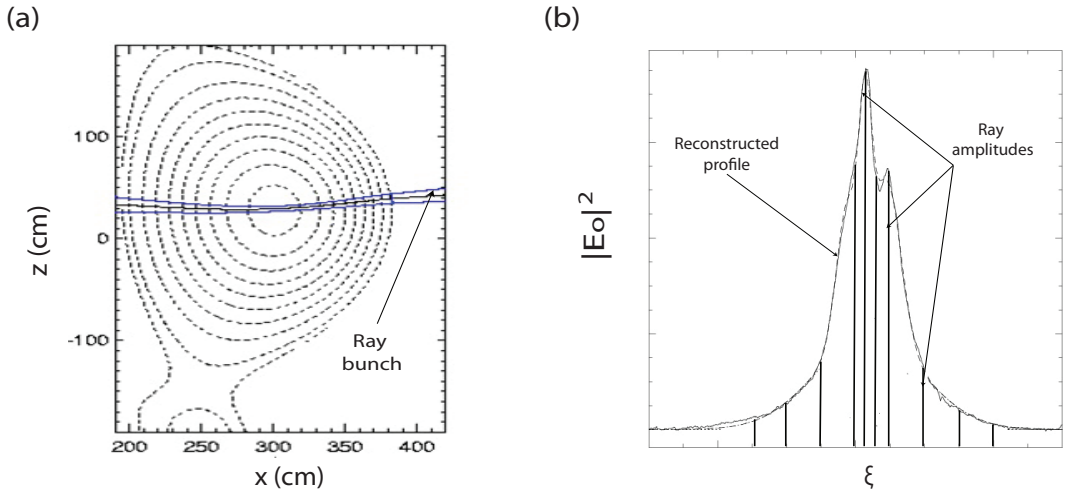

Figure 3: (a) Illustration of the beam representation in terms of propagating wave rays. (b) Beam electric field amplitude reconstruction by the amplitudes of rays set spatially dense across propagation.

beam contour, which sum up to the expected electric field profile across propagation. Assuming that the rays have amplitudes $\overline{C}_m$, polarization vectors $\bar{\mathbf{e}}_\mathbf{m}$ and generalized (eikonal) phases s_m along the propagation paths defined by the position vectors $\mathbf{r_m}$, where all these quantities are known from the solution of the corresponding Hamiltonian ray and amplitude transport equations, the arbitrary electric field has the form

$$\overline{\mathbf{E}}(\mathbf{r}) = \sum_m \delta(\mathbf{r} - \mathbf{r_m}) \overline{C}_m(\mathbf{r}) \exp\left[i\kappa s_m(\mathbf{r})\right] \bar{\mathbf{e}}_\mathbf{m}(\mathbf{r}). \tag{20}$$

The above expression is actually a discrete approximation of the beam over locally plane waves, contrary to the updated paraxial beam tracing technique described previously where the discretization aims to the employment of different orders of generalized Gaussian modes. Using rays, the requirements for achieving accuracy in the approximation are different regarding the beam extent and the amplitude profile: The correct description of the beam extent relies mainly on the proper modeling of the few rays neighbouring to the beam transverse borders, whereas a large number of rays is required to describe sufficiently the electric field profile, in order to provide amplitude values densely within the region enclosed by the bordering rays.

In Figure 3 the details of the beam approximation via asymptotic rays are illustrated. In comparison to beam tracing, the ray-based description does not provide a detailed computation of diffractive or interference effects on the beam extent, because, as it stands for geometric optics, the propagation of each ray the beam is composed of is calculated independently, not influenced by its neighbouring rays. In the amplitude description, the method based on rays may have a better performance in the modeling of extremely asymmetric beams, e.g. due to truncation induced by inhomogeneous power absorption or partial reflection, however the number of modes required for achieving good accuracy is much more increased with respect to beam tracing.

4 Generalization of the Gaussian beam parametrization

In the majority of studies involving wave beams in applied optics, the propagating beams are considered to be of Gaussian shape, although this is a (at least) desirable situation in some cases. In terms of optics, Gaussian beams are preferable because they appear smoother propagation and are easier to model. For applications relevant to fusion, Gaussian beams provide enhanced spatial localization and thus "surgical" accuracy in plasma perturbation plus more reliable measurements [22]. In order to be able to take advantage of the extensive knowhow available on the symmetric beam description, the notion of the parameters relevant to the Gaussian beam has to be refined. This is necessary, because for arbitrary beams the standard definitions are inadequate since, in most cases, they underestimate the contour size of the beam and/or provide a misleading picture of the wavefront boundary.

In the context of paraxial beam tracing, the width W, the divergence angle Θ_0 and the curvature radius of the wavefront R_C of an arbitrary beam may be generalized on the basis of the distribution of the electric field amplitude $\overline{E}$ per direction ξ_j $(j = 1, 2)$ transverse to the propagation. The specific formulas are [23]

$$\widetilde{W}_j^2 = \frac{\int_{-\infty}^{+\infty} \xi_j^2 |\overline{E}|^2 d\xi_1 d\xi_2}{\int_{-\infty}^{+\infty} |\overline{E}|^2 d\xi_1 d\xi_2} - \left(\frac{\int_{-\infty}^{+\infty} \xi_j |\overline{E}|^2 d\xi_1 d\xi_2}{\int_{-\infty}^{+\infty} |\overline{E}|^2 d\xi_1 d\xi_2} \right)^2, \tag{21a}$$

$$\widetilde{\Theta}_{0,j}^2 = \frac{\int_{-\infty}^{+\infty} \psi_j^2 |\overline{\mathcal{E}}|^2 d\psi_1 d\psi_2}{\int_{-\infty}^{+\infty} |\overline{\mathcal{E}}|^2 d\psi_1 d\psi_2} - \left(\frac{\int_{-\infty}^{+\infty} \psi_j |\overline{\mathcal{E}}|^2 d\psi_1 d\psi_2}{\int_{-\infty}^{+\infty} |\overline{\mathcal{E}}|^2 d\psi_1 d\psi_2} \right)^2, \tag{21b}$$

$$\frac{\widetilde{W}_j^2}{\widetilde{R}_{C,j}} = \frac{\int_{-\infty}^{+\infty} \xi_j \left(\overline{E}\overline{E}_j^{\star\prime} - \overline{E}_j' \overline{E}^{\star} \right) d\xi_1 d\xi_2}{\int_{-\infty}^{+\infty} |\overline{E}|^2 d\xi_1 d\xi_2} + \frac{\int_{-\infty}^{+\infty} \xi_j |\overline{E}|^2 d\xi_1 d\xi_2}{\int_{-\infty}^{+\infty} |\overline{E}|^2 d\xi_1 d\xi_2} \frac{\int_{-\infty}^{+\infty} \psi_j |\overline{\mathcal{E}}|^2 d\psi_1 d\psi_2}{\int_{-\infty}^{+\infty} |\overline{\mathcal{E}}|^2 d\psi_1 d\psi_2}, \tag{21c}$$

with ψ, $\overline{\mathcal{E}}$ being the Fourier transforms of ξ, $\overline{E}$, $\overline{E}^{\star}$ being the complex conjugate of $\overline{E}$, the primes referring to differentiation over ξ_j, and the tilde denoting normalization over the corresponding values of the Gaussian mode. It is clear that W and Θ_0 are formed by the moments of the amplitude distribution of the field and of its Fourier transform, while R_C additionally invokes the slope across propagation and the field polarization.

With the expression of Equation (13) for the electric field, the calculation of the generalized beam parameters from (21) is straightforward. Considering the beam field as the sum of the purely Gaussian (zero-order) term plus all the higher-order modes, i.e. $\overline{E} = \overline{E}_{0,0} + \sum_{m,n} \overline{E}_{m,n}$, the beam-tracing ansatz reaches a compact form

$$\overline{E} = \overline{C}_{0,0} \exp[i(\kappa s - \Theta_{0,0})] \exp\left[-\frac{\xi_1^2 + \xi_2^2}{2} \right] \left[1 + \sum_{m,n} \bar{c}_{m,n} \exp\left(-i\Theta_{m,n}\right) H_m(\xi_1) H_n(\xi_2) \right], \tag{22}$$

where $\bar{c}_{m,n} = \overline{C}_{m,n} / \overline{C}_{0,0}$ is the ratio of the amplitude of the higher-order mode (m, n) over the amplitude of the Gaussian mode. The square of the electric field $|\overline{E}|^2 = \overline{E} \cdot \overline{E}^*$ can

then be expressed as follows

$$|\overline{E}|^2 = |\overline{C}_{0,0}|^2 \exp\left(-\xi_1^2 - \xi_2^2\right) \Bigg[1 + \sum_{m,n} |\bar{c}_{m,n}|^2 H_m^2(\xi_1) H_n^2(\xi_2) + 2 \sum_{m,n} |\bar{c}_{m,n}| \cos\theta_{m,n} H_m(\xi_1) H_n(\xi_2) + \sum_{m,n,k,l} |\bar{c}_{m,n}||\bar{c}_{k,l}| \cos(\theta_{m,n} - \theta_{k,l}) H_m(\xi_1) H_n(\xi_2) H_k(\xi_1) H_l(\xi_2) \delta'_{m,k,n,l} \Bigg]. \quad (23)$$

In Equation (23), the angle $\theta_{m,n} = \Theta_{m,n} - \Theta_{0,0} - \arg(\bar{c}_{m,n})$ is the total phase shift due to the complex part of the beam amplitude plus the different group velocity of each propagating mode, and the term $\delta'_{m,k,n,l} = 1 - \delta_{m,k}\delta_{n,l}$ invokes Kronecker delta symbols for switching on/off the presence of specific coupling terms.

According to the above, the moments of $|\overline{E}|^2$ (required for deriving all the beam parameters) may be calculated analytically. The result for the zero-order moment is

$$\Xi^0 = |\overline{C}_{0,0}|^2 \left(1 + \sum_{m,n} |\bar{c}_{m,n}|^2 \right), \quad (24)$$

and the calculation for the higher-order moments relevant to ξ_1 yields [18]

$$\Xi_1^1 = |\overline{C}_{0,0}|^2 \sum_{m,n,k,l} |\bar{c}_{m,n}||\bar{c}_{k,l}| \cos(\theta_{m,n} - \theta_{k,l}) \delta_{n,l} \left(\sqrt{\frac{m}{2}} \delta_{m,k+1} + \sqrt{\frac{k}{2}} \delta_{m,k-1} \right) + 2|\overline{C}_{0,0}|^2 \sum_{m,n} |\bar{c}_{m,n}| \cos\theta_{m,n} \sqrt{\frac{m}{2}} \delta_{m,1} \delta_{n,0}, \quad (25a)$$

$$\Xi_1^2 = |\overline{C}_{0,0}|^2 \sum_{m,n,k,l} |\bar{c}_{m,n}||\bar{c}_{k,l}| \cos(\theta_{m,n} - \theta_{k,l}) \delta_{n,l} \cdot \left[\sqrt{m(m-1)} \delta_{m,k+2} + \sqrt{k(k-1)} \delta_{m,k-2} \right] + |\overline{C}_{0,0}|^2 \left[1 + \sum_{m,n} |\bar{c}_{m,n}|^2 + 2 \sum_{m,n} |\bar{c}_{m,n}| \cos\theta_{m,n} \sqrt{m(m-1)} \delta_{m,2} \delta_{n,0} \right], \quad (25b)$$

The same moments for the second transverse coordinate may be found easily from the above by interchanging the subscripts (m, k) with (n, l), whereas the moments Ψ of the Fourier-transformed field $\overline{\mathcal{E}}$, corresponding to the "angles" ψ, emanate from the moments Ξ by changing the sign in front of every cosine in (25).

A direct comparison of Equations (24) and (25) with the definitions in (21) shows that the generalized beam width and divergence must be given by

$$\widetilde{W}_j = \sqrt{\frac{\Xi_j^2}{\Xi^0} - \left(\frac{\Xi_j^1}{\Xi^0} \right)^2}, \quad (26a)$$

$$\widetilde{\Theta}_{0,j} = \sqrt{\frac{\Psi_j^2}{\Psi^0} - \left(\frac{\Psi_j^1}{\Psi^0} \right)^2}, \quad (26b)$$

whereas, regarding the radius of curvature of the wavefront, straightforward calculus yields the relation $\int_{-\infty}^{+\infty} \xi_j \left(\overline{EE}_j^{\star\prime} - \overline{E}_j^{\prime} \overline{E}^{\star} \right) d\xi_1 d\xi_2 = \Xi_j^2 \Psi_j^1 - \Xi_j^1 \Psi_j^2$, which correlates the integral with the amplitude distributions, and therefore one finally obtains for R_C a result in the same context with W and Θ_0

$$\widetilde{R}_{C,j} = \frac{\Xi^0 \Psi^0}{\Xi^0 (\Xi_j^2 \Psi_j^1 - \Xi_j^1 \Psi_j^2) + \Xi_j^1 \Psi_j^1} \widetilde{W}_j^2. \tag{27}$$

In the framework of the ray tracing method, the formulation described previously cannot be directly applied because each ray is actually a locally plane wave, and, consequently, it defines a value of the wave amplitude on a single point rather than a transverse profile. This is verified by looking at Equation (20), where an explicit dependence on other coordinates than the one along the ray propagation path does not exist. Therefore, here, the generalized parameters will be calculated in terms of the trajectories and the amplitudes (relevant to the carried fraction of wave power) of the ensemble of rays constituting the beam, using the standard parameter definitions. This calculation is performed by integrating the ray equations with proper initial conditions, such that the beam extent and the wavefront are implicitly simulated.

Assuming that the central ray of the beam is on the position vector $\mathbf{r_0}$ and the peripheral rays defining the beam boundary are on the vectors $\mathbf{r}_{+,\mathbf{j}}$ and $\mathbf{r}_{-,\mathbf{j}}$, the beam widths may be defined as the distances between the peripherals (actually the line segments connecting $\mathbf{r_0}$ and the tangential vectors $d\mathbf{r}_{+,\mathbf{j}}/d\tau$, $d\mathbf{r}_{-,\mathbf{j}}/d\tau$ on these points)

$$W_j(\tau) = \frac{1}{2} \left| \mathbf{r}_{+,\mathbf{j}}(\tau) - \mathbf{r}_{-,\mathbf{j}}(\tau) \right|. \tag{28}$$

Having completed the calculation of the values of the beam width along the propagation, the divergence angle per direction may be computed in terms of its standard definition as the angular measure of the increase of the beam transversal extent as it propagates away from the initial (launch) point [24]

$$\Theta_{0,j}(\tau) = \arctan \left[\frac{W_j(\tau) - W_j(0)}{|\mathbf{r_0}(\tau) - \mathbf{r_0}(0)|} \right]. \tag{29}$$

Finally, regarding the wavefront curvature, one again resorts to the classical definition: The wavefront is the geometrical locus of all the points along propagation that have the same wave phase, and, in general, it is an approximately spherical curve of some radius. In our problem, at each propagation instant defined by τ, this involves the point $\rho_{\mathbf{m},\mathbf{j}}(\tau)$ from each ray that has a phase equal to the eikonal phase $s_0(\tau)$ on the central ray. Having calculated and stored these M points, one approximates the curvature radius as their mean distance from the launch point, taking also into account, in its sign, the focusing/defocusing region of the beam in terms of the width derivative

$$R_{C,j}(\tau) = \text{sign} \left[\frac{dW_j(\tau)}{d\tau} \right] \frac{1}{M} \sum_m \left| \rho_{\mathbf{m},\mathbf{j}}(\tau) - \rho_{\mathbf{m},\mathbf{j}}(0) \right|. \tag{30}$$

5 Numerical application

As an application for illustrating the capabilities of the above formalisms, the case of O-mode electron-cyclotron beam propagation in a stratified, cold magnetized plasma is

treated. The medium is confined in the region $-a \leq X \leq a$ along the $X-$axis, while it runs unlimited in the other directions Y, Z of the laboratory frame. In the following, all the lengths are normalized to α and the wave-vectors to the vacuum wave-vector ω/c, and the lab frame coordinates in their dimensionless form read $(x, y, z) = (X/a, Y/a, Z/a)$. All the plasma properties are assumed to be functions only of the $x-$coordinate. The static magnetic field is along the $z-$axis, and the wave beam is launched from the low-field side at $X = X_0 = a$ in the negative $x-$direction, i.e. $k_y(x_0) = k_z(x_0) = 0$. In this context, τ is a function of x only and the normalized transverse coordinates describing the amplitude profile are y/w_y and z/w_z, where w_y, w_z are the normalized principal (Gaussian) widths in each perpendicular direction.

An analytic solution of the equations for ray tracing and paraxial beam tracing for this problem has been obtained in [25]. The simplification here is that the dispersion (Hamiltonian) function reduces to a quadratic form in Cartesian coordinates [8],

$$D = \sum_{\alpha} \frac{1}{2} D^M_{\alpha,\alpha} k^2_\alpha - \frac{1}{2} = 0, \tag{31}$$

and yields simple ray tracing equations ($M = O, X$ indicates the polarization mode)

$$\frac{dx_\alpha}{d\tau} = \frac{\partial D}{\partial k_\alpha} = D^M_{\alpha,\alpha} k_\alpha, \tag{32a}$$

$$\frac{dk_\alpha}{d\tau} = -\frac{\partial D}{\partial x_\alpha} = \frac{1}{2} \frac{\partial D^M_{\alpha,\alpha}}{\partial x_\alpha} k^2_\alpha. \tag{32b}$$

In the above, D does not depend on y, z, and hence the wave-vectors k_y, k_z are constantly zero throughout the propagation.

The complex tensor $\bar{s}_{\alpha,\beta}$, formed as a result of the paraxial expansion (see again Section 2), is also diagonal in the simplified geometry

$$\bar{s}_{\alpha,\alpha}(x) = \frac{\bar{s}_{\alpha,\alpha}(x_0)}{1 + \bar{s}_{\alpha,\alpha}(x_0)\zeta_\alpha(x)}, \tag{33}$$

where the effective lengths ζ_α are defined by the relations

$$\zeta_\alpha(x) = \int_0^\tau D^M_{\alpha,\alpha}(\tau')d\tau' = -\int_{x_0}^{x} \frac{D^M_{\alpha,\alpha}(x')}{\sqrt{D^M_{x,x}(x')}} dx'. \tag{34}$$

If Equation (33) is expressed in terms of the real and imaginary parts of $\bar{s}_{\alpha,\alpha} = s_{\alpha,\alpha} + i\phi_{\alpha,\alpha}$ and the corresponding initial values, it provides the solution of the beam tracing equations for the wavefront curvature ($r_{c,a} = \kappa^{-1}/s_{\alpha,\alpha}$) and the width ($w_a^2 = 2\kappa^{-1}/\phi_{\alpha,\alpha}$). A straightforward manipulation yields

$$s_{\alpha,\alpha}(x) = \frac{s_{\alpha,\alpha}(x_0) + \left[s^2_{\alpha,\alpha}(x_0) + \phi^2_{\alpha,\alpha}(x_0)\right]\zeta_\alpha(x)}{\left[1 + s_{\alpha,\alpha}(x_0)\zeta_\alpha(x)\right]^2 + \left[\phi_{\alpha,\alpha}(x_0)\zeta_\alpha(x)\right]^2}, \tag{35a}$$

$$\phi_{\alpha,\alpha}(x) = \frac{\phi_{\alpha,\alpha}(x_0)}{\left[1 + s_{\alpha,\alpha}(x_0)\zeta_\alpha(x)\right]^2 + \left[\phi_{\alpha,\alpha}(x_0)\zeta_\alpha(x)\right]^2}. \tag{35b}$$

For waves with O-mode polarization, the tensor elements are $D^O_{\alpha,\alpha} = (\delta_{\alpha,x} + \delta_{\alpha,y})/P + \delta_{\alpha,z}$ [8], where $P = 1 - \omega_p^2/\omega^2$ is a dimensionless parameter determined by the plasma density profile. In our simple, geometrically stratified case, we assume a parabolic profile of the form $P(x) = p_1 + p_2 x^2$. As a consequence, the effective lengths may be directly evaluated using lookup tables of integrals (e.g. [20])

$$\zeta_y(x) = \frac{1}{\sqrt{p_2}} \ln\left(\frac{\sqrt{p_2} + \sqrt{p_1 + p_2}}{x\sqrt{p_2} + \sqrt{p_1 + p_2 x^2}}\right), \tag{36a}$$

$$\zeta_z(x) = \frac{1}{2}\left[\sqrt{p_1 + p_2} - x\sqrt{p_1 + p_2 x^2}\right] + \frac{1}{\sqrt{p_2}} \ln\left(\frac{\sqrt{p_2} + \sqrt{p_1 + p_2}}{x\sqrt{p_2} + \sqrt{p_1 + p_2 x^2}}\right). \tag{36b}$$

Finally, regarding the phase difference θ_{mn} of the modes, it is given by

$$\theta_{m,n}(x) = -\arg[\bar{c}_{m,n}(x)] + m\int_{x_0}^{x} D^M_{y,y}(x')\phi_{y,y}(x')dx' + n\int_{x_0}^{x} D^M_{z,z}(x')\phi_{z,z}(x')dx'. \tag{37}$$

Especially for this case where wave-particle absorption does not occur, the amplitude ratios $\bar{c}_{m,n}$ do not vary along the propagation path. This is a direct consequence of the energy conservation, as expressed in the version of (7) with zero absorption coefficient γ. In such cases, this equation is exactly the same for all propagating modes, and therefore all the amplitudes $\overline{C}_{m,n}$ scale as the same function of x along the propagation path. In this paper we will not deal further with the amplitude transport; for a more detailed treatment of this issue, the reader is pointed to [18].

In the following, indicative results are presented from the numerical solution of the problem for non-Gaussian input, based on the asymptotic solutions and the generalizations of the beam parameters presented in the previous sections. A small computer code was built for the calculation of the widths W_j, w_j and all the other relevant parameters, to which the user should provide as input the half-width a of the plasma slab, the mode numbers m, n of the higher-order modes, the initial beam widths and radii of curvature, the parameters p_1, p_2 for the parabolic profile of the plasma frequency, and also the ratios $\epsilon_{m,n}$ of the power corresponding to the extra modes over the total wave power. These ratios are connected to the amplitude ratios through the relation

$$\epsilon_{m,n} = \frac{|\bar{C}_{m,n}|^2}{|\bar{C}_{0,0}|^2 + |\bar{C}_{m,n}|^2} = \frac{|\bar{c}_{m,n}|^2}{1 + |\bar{c}_{m,n}|^2}, \tag{38}$$

and one can distinguish the connection between the distribution of the beam energy among the different modes and the geometry of the beam.

The input and output values of the program are expressed in physical units, and any normalization needed is performed in the routine part of the code. For the results in this application, the fixed parameters have the following values: The half-width of the plasma slab is $a = 100$ cm, the wave frequency is $\omega/2\pi = 140$ GHz (near the cyclotron frequency), the zero-order (Gaussian) mode $\overline{E}_{0,0}$ has a circularly symmetric initial amplitude profile with principal widths $w_y(x_0) = w_z(x_0) = 4.27$ cm, as well as a symmetric initial beam focusing with principal curvature radii $r_y(x_0) = r_z(x_0) = -82$ cm, the scaling parameters for the plasma frequency radial profile are $c_1 = 0.9$, $c_2 = 0.5$, and the short-wavelength limit parameter is $\kappa = \omega\alpha/c = 2932.15$. We should also note that we have chosen the modes to have the same initial polarization, and as a result $\arg(\bar{c}_{m,n})$ is constantly zero throughout the beam propagation.

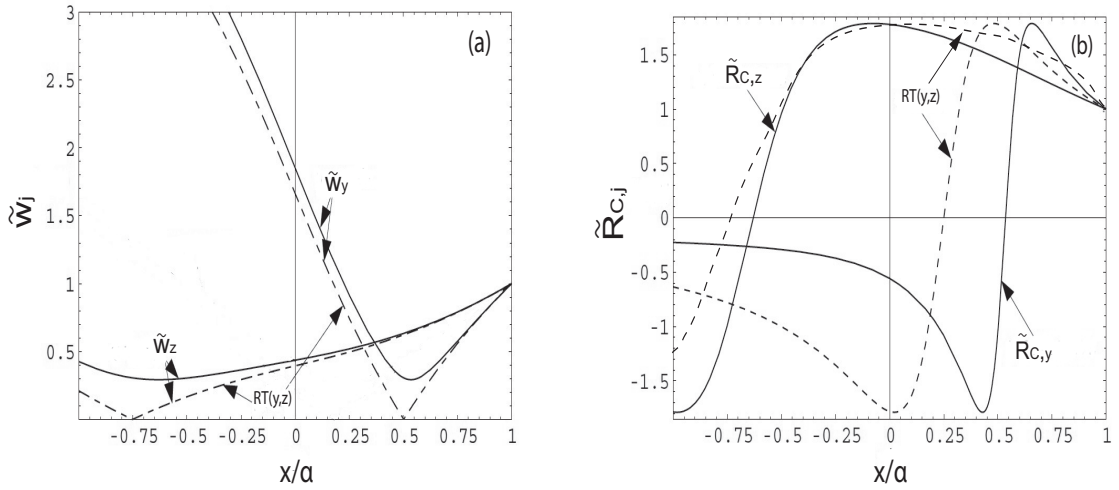

Figure 4: (a) Generalized beam width along propagation in a stratified anisotropic plasma as predicted by the ray and beam tracing techniques. (b) Generalized wavefront curvature radius vs propagation path in the stratified anisotropic plasma as predicted by the ray and beam methods.

In Figure 4, the generalized beam coordinates in both transverse directions y, z are shown as a function of the propagation path coordinate x, for the case of a non-Gaussian beam generated by perturbing a Gaussian beam with only one Hermite mode of order $(m, n) = (1, 2)$, and an energy deposit on the higher-order term equal to $\epsilon_{m,n} = 0.05$. Regarding the width, one can see that the beam tracing result, which incudes diffraction in the description, yields that the beam reaches a minimum of finite size, whereas the ray tracing estimation presents an unphysical focus as a minimum. It is also apparent that the beam behaviour is different in the two directions, which means that the initial symmetry of the beam contour has disappeared. This effect is owed to the presence of the magnetic field (in the direction z), which induces a strong anisotropy in the plasma and, accordingly, an astigmatic behaviour to the beam.

6 Conclusions

In this work, we presented a way of extending the state-of-the-art in asymptotic wave methods in order to be able to model the evolution of arbitrary wave beam structures. The sequence breaks down to the decomposition of the beam propagation into the one of properly configured ray/beam modes, and, following that, the generalization of the typical Gaussian beam parameters into a new scheme capable of describing arbitrary beam profiles under the same context. As an instructive application, we followed the propagation of a non-Gaussian high-frequency beam in a bounded plasma with simple magnetic geometry, a case where an analytic solution of the problem (and thus a highly-trackable benchmark) is possible.

A feasible application of the above is the extension of asymptotic ray/beam tracing codes to include the propagation of arbitrary beams and assessment in further computations, like e.g. the consistent description of the propagation, absorption and current drive of arbitrary beams in a tokamak plasma. Apart from the evolution of more complex wave objects, the study of non-Gaussian beams is also important for the improvement of the modelling of the wave power absorption in the plasma, by describing modifications of the

profile shape due to localized asymmetric and/or inhomogeneous absorption in terms of the generation of higher-order modes which exchange energy.

Acknowledgement

This work has been supported by (a) the National Programme for the Controlled Thermonuclear Fusion, Hellenic Republic, (b) the EJP Cofund Action SEP-210130335 EUROfusion. The sponsors do not bear any responsibility for the content of this work.

References

[1] D. G. Swanson, *Plasma Waves* (Academic, New York, 1989)

[2] L. Friedland, I. B. Bernstein, *Phys. Rev. A* **22** (1980) 1680

[3] E. Mazzucato, *Phys. Fluids B* **1** (1989) 1855

[4] A. Bravo-Ortega, A. H. Glasser, *Phys. Fluids B* **3** (1991) 529

[5] G. Pereverzev, *Phys. Plasmas* **5** (1998) 3529

[6] Yu. A. Kravtsov and Yu. I. Orlov, *Geometrical Optics of Inhomogeneous Media* (Springer Verlag, Berlin, 1990)

[7] L. D. Landau, E. M. Lifshitz, *The Classical Theory of Fields* (Pergamon Press, Oxford, 1997)

[8] T. H. Stix, *Waves in Plasmas* (McGraw-Hill, New York, 1992)

[9] E. Westerhof, Technical Report 89, FOM-Rijnhuizen (1989)

[10] E. Poli, A. G. Peeters, G. Pereverzev, *Comp. Phys. Commun.* **136** (2001) 90

[11] D. Farina, Technical Report FP 05/1, IFP-CNR (2005)

[12] V. Erckmann, U. Gasparino, *Plasma Phys. Control. Fusion* **36** (1994) 1869

[13] R. Prater, *Phys. Plasmas* **11** (2004) 2349

[14] C. Tsironis, A. G. Peeters, H. Isliker, D. Strintzi, I. Chatziantonaki, L. Vlahos, *Phys. Plasmas* **16** (2009) 112510

[15] R. Kamendje, S. V. Kasilov, W. Kernbichler, M. F. Heyn, *Phys. Plasmas* **10** (2003) 75

[16] C. Tsironis, L. Vlahos, *Plasma Phys. Control. Fusion* **47** (2005) 131

[17] B. Lloyd, *Plasma Phys. Control. Fusion* **40** (1998) A119

[18] C. Tsironis, E. Poli, G. Pereverzev, *Phys. Plasmas* **13** (2006) 113304

[19] C. Tsironis, *PIER B* **47** (2012) 37

[20] G. B. Arfken, H. J. Weber, *Mathematical Methods for Physicists (2nd Ed.)* (Academic, New York, 1995)

[21] M. Bornatici, *Nucl. Fusion* **23** (1983) 1153

[22] K. K. Kirov, F. Leuterer, G. Pereverzev, F. Ryter, W. Suttrop, the AUG team, Technical Report 02/9, MPI-IPP (2002)

[23] M. A. Porras, J. Alda, E. Bernabeu, *Appl. Optics* **31** (1992) 6389

[24] A. E. Siegman, *Lasers* (University Science, Boston, 1986)

[25] E. Poli, G. Pereverzev, A. G. Peeters, *Phys. Plasmas* **6** (1999) 5